Modelling of fast neutral Li beams for fusion edge plasma diagnostics

1999 Plasma Phys. Control. Fusion 41 471

(http://iopscience.iop.org/0741-3335/41/4/002)

Plasma Phys. Control. Fusion **41** (1999) 471–484. Printed in the UK PII: S0741-3335(99)99426-5

Modelling of fast neutral Li beams for fusion edge plasma diagnostics

R Brandenburg†, J Schweinzer‡, S Fiedler‡, F Aumayr† and HP Winter†§

† Institut für Allgemeine Physik, TU Wien, Association EURATOM-OEAW, A-1040 Wien, Austria

‡ Max-Planck-Institut für Plasmaphysik, EURATOM Association, D-85748 Garching, Germany

Received 17 November 1998, in final form 25 January 1999

Abstract. We present an experimental and theoretical study on the modelling of fast (5 keV amu^{-1}) Li beams which are used for diagnostics of fusion edge plasmas. The atomic collision database utilized for modelling the Li beam attenuation has been revised and extended by detailed investigations of Li(nl; $n \geqslant 3$) populations resulting from ion impact excitation. We obtain good agreement between measured and calculated Li(nl) populations for an Li beam passing the edge plasma region of the ASDEX Upgrade tokamak and WENDELSTEIN 7 AS stellarator, respectively, at IPP Garching.

1. Introduction

Edge plasma properties and impurity transport phenomena are intimately linked with the plasma–wall interaction of thermonuclear fusion plasmas. A fast neutral Li beam injected into the plasma provides a powerful edge plasma diagnostic method which has reached a satisfactory standard in recent years [1, 2]. Li beam plasma spectroscopy is now a reliable method for reconstructing electron density profiles from the line radiation of collisionally excited Li atoms (Li beam impact excitation spectroscopy, Li-IXS) [3, 4]. In addition, impurity ion concentration and temperature profiles can be obtained from impurity ion line emission stimulated by electron capture from injected Li atoms (Li beam charge exchange spectroscopy, Li-CXS) [5, 6].

Utilization of these diagnostic capabilities requires an extensive database including all relevant collisional processes of Li atoms with plasma particles (i.e. electrons, protons and impurity ions). In particular, the population of higher Li(nl) states needs to be described rather accurately since the efficiency of electron capture from the injected Li atoms depends strongly on the relative amount of these Li(nl) states.

In order to check the accuracy of our present beam modelling and the underlying database, experimental investigations of the composition of diagnostic Li beams utilized at IPP Garching have been carried out by observing Li(2p $\rightarrow$ 2s; 3d $\rightarrow$ 2p; 4s $\rightarrow$ 2p; 4d $\rightarrow$ 2p) line radiation profiles. The experimental set-up of lithium beam diagnostics on both fusion devices at IPP Garching (the ASDEX Upgrade tokamak and the WENDELSTEIN 7 AS (W7-AS) stellarator) as well as the way to observe Li(nl) populations has already been described elsewhere [1, 7, 8].

§ Corresponding author. E-mail address: winter@iap.tuwien.ac.at

0741-3335/99/040471+14$19.50

We found large discrepancies between predictions of the current beam modelling and experimental investigations regarding Li(nl; $n \geqslant 3$) populations, which clearly exceeded the experimental errors involved (cf the typical example in figure 1).

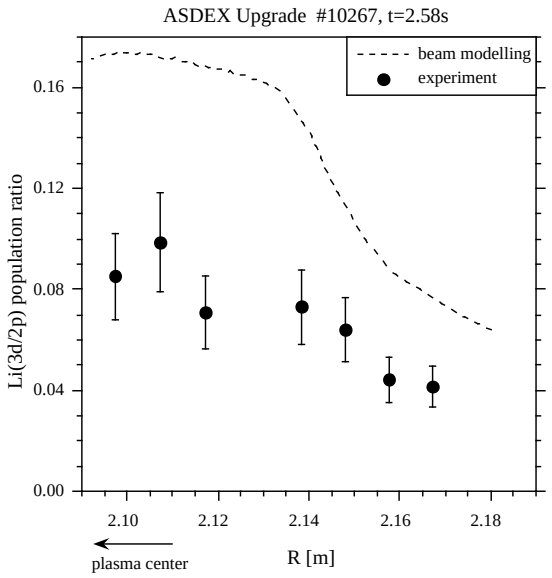

Figure 1. The ratio of Li(3d) and Li(2p) populations along the beam path in an ASDEX Upgrade discharge. While the calculated ratio strongly increases with increasing beam penetration depth, the experimental results remain considerably lower.

As the main reason for these deviations, we suspected inaccurate cross sections in the database which contains data for electron and ion impact ionization, electron and ion impact excitation, and electron capture. Therefore, we have thoroughly examined our database and systematically investigated the effects of various datasets and modelling details on the Li excitation processes.

In section 2 we will describe the status of the current database, including a detailed presentation of theoretical and experimental determination of cross sections for ion impact on Li as well as a brief overview of available cross sections for electron impact. In section 3 we will compare experimental results regarding the composition of a diagnostic Li beam with our beam modelling. We will also present the effects of the improved modelling on the determination of electron and impurity ion densities. In section 4 we will finally discuss the necessary size of the modelling algorithm and the underlying database.

2. Determination of Li proton impact excitation cross sections

Regarding collisions between Li atoms and plasma ions (in particular hydrogen ions) the currently used database [9] contains only a few measured or *ab initio* calculated cross sections. Whereas there are sufficiently reliable experimental and calculated data for ionization and electron capture processes in H^+–Li collisions, excitation processes due to the impact of heavier ions have not been investigated in similar detail until now. In particular, there has been a lack of data for ion impact excitation into higher Li(nl; $n \geqslant 3$) states which so far had been derived by scaling from the respective electron impact excitation cross sections. Due to improved computing capabilities we are now able to calculate all proton induced transitions

within the Li(nl; $n \leqslant 4$) states. In order to check these calculations we have also carried out experimental investigations of the important Li(2s $\rightarrow$ 3d) excitation which will be presented in the following section. Following these refined calculations, all excitation cross sections for Li(2s $\rightarrow$ nl; $n \geqslant 3$) and for Li(2p $\rightarrow$ nl; $n \geqslant 3$) have become considerably smaller than the data contained in the utilized database so far, in some cases by up to a factor of five. These results will be collected in a new database which will be published elsewhere [10].

2.1. Experimental technique

In order to support and check our new theoretical excitation cross sections (cf section 2.2) for ion impact, the excitation process Li(2s $\rightarrow$ 3d) which provides an important contribution to the population of Li(nl; $n = 3$) states has been investigated experimentally by means of absolute photon-spectroscopic measurements of the corresponding Li I radiation at $\lambda = 610.4$ nm.

We used a crossed-beam apparatus (figure 2) similar to the one described in [11] and [12]. Projectile ions (H^+, He^+) were extracted from a 2.45 GHz electron cyclotron resonance (ECR) ion source [13].

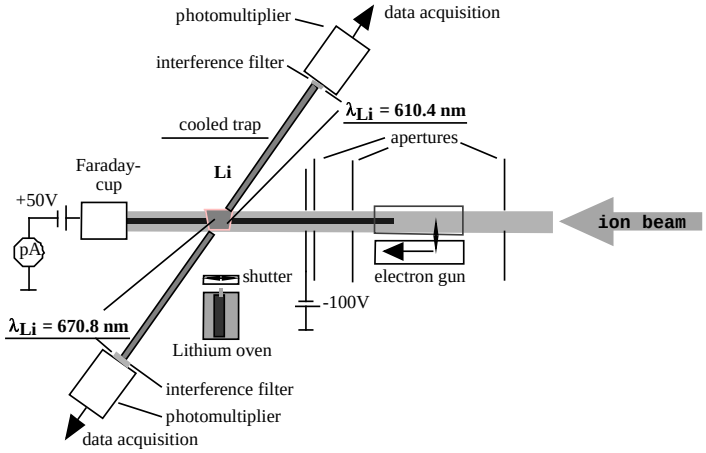

Figure 2. Experimental set-up for simultaneous measurements of Li I(3d $\rightarrow$ 2p) and Li I(2p $\rightarrow$ 2s) radiation following ion and electron impact, respectively.

The Li I(3d $\rightarrow$ 2p) emission has been calibrated to simultaneously measured, already well known Li I(2p $\rightarrow$ 2s) data [11]. Li I line radiation (670.8 nm; 610.4 nm) from the ion–atom interaction region was detected by two cooled photomultipliers with interference filters (EMI 9816 QB with Schott type MA 7-0.5, and EMI 9659 QB photomultiplier with Laser Components LC-610.4NB1.0-50, respectively). A possible polarization-related anisotropy of the emitted line radiation was taken care of by viewing under the 'magic' angle of 54.7° with respect to the ion beam axis. The observation length of the photon detection system was confined by slits to 6.5 mm along the ion beam axis, in order to reduce background from the excitation of residual gas molecules, scattered Li atoms and black-body radiation from the Li oven.

Relative values of the Li I emission cross sections were determined with respect to the reference impact energy of 10 keV. The set-up was absolutely calibrated by measuring the respective line emission due to impact of electrons ($E = 300$ eV) instead of ions. For this purpose we applied a moveable electron gun and a set of apertures to assure similar interaction geometries for the electron and ion beams. Electron impact excitation cross sections were taken

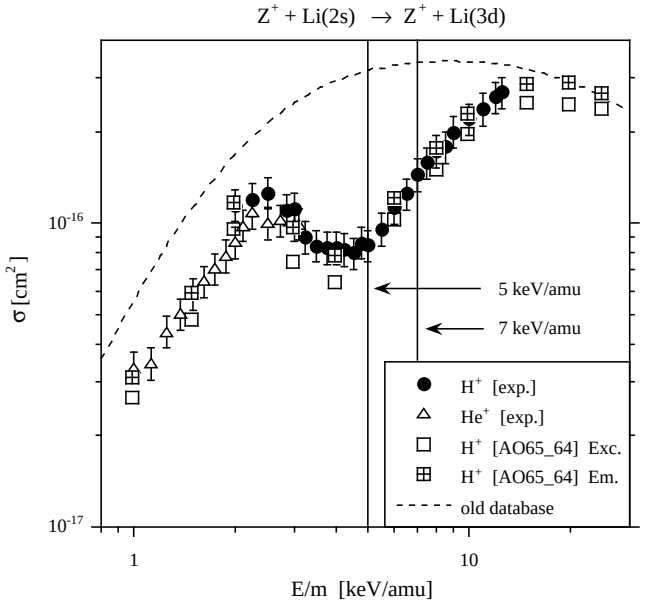

Figure 3. Measured and calculated Li I(3d → 2p) emission cross sections. While measured He^+ data are slightly lower than H^+ data in the overlapping region, both agree quite satisfactorily with the corresponding calculations. The cross sections from the old database, which were scaled from respective electron collisions, do not show any structure. The AO-CC calculation also delivers Li(2s → 3d) excitation cross sections ('Exc.'). The two vertical lines indicate Li beam energies of 35 and 48 keV as applied on ASDEX Upgrade and W7-AS, respectively. In the case of ASDEX Upgrade the new cross sections differ from the old ones by a factor of 3.7.

from [14]. Calculating the ratio of the simultaneously measured line emissions Li I(3d → 2p) and Li I(2p → 2s) minimized errors due to Li target density fluctuation.

Statistical errors of our relative cross sections, which are mainly caused by reproducibility, are typically less than ±5% for ion impact and up to ±10% for electron impact. In addition, a quoted error of ±10% for the Li(2s → 2p) proton impact excitation cross section [11] was taken into account, leading to total errors in the range of ±15% (table 1). Our measured cross sections of Li I(2p → 2s) and Li I(3d → 2p) emission differ from the related Li I(2p) and Li I(3d) excitation cross sections because of cascades to Li(2p) and Li(3d) from higher excited Li(nl; $n \geqslant 3$) levels (cf equations (1) and (2) in section 2.2).

2.2. Results and comparison with theory

The measured Li(2s → 3d) cross sections for H^+ and He^+ ion impact excitation are given in figure 3. They show a characteristic undulatory structure with a local minimum at $E \approx 4$ keV amu^{-1} and a local maximum at $E \approx 2$ keV amu^{-1}. Similar structures have already been observed for Li(2s → 2p) excitation by impact of multiply-charged ions and explained by the competing electron capture channel [12] and the interplay between two separate excitation mechanisms [15]. Measured data for He^+ ions are slightly lower than for H^+ in the overlapping impact energy region (cf table 1), which is also the case for Li(2s → 2p) excitation [16]. This can be explained by the fact that single electron capture is relatively more important for He^+ than for H^+ impact.

Experimental results were compared to atomic-orbital close-coupling (AO-CC)

Table 1. Measured Li(3d → 2p) emission cross sections and errors.

	E/m (keV amu^{-1})	σ (cm^2)	$\Delta\sigma/\sigma$ (±%) abs.
H^+	2.00	1.14×10^{-16}	23.4
	2.25	1.19×10^{-16}	20.7
	2.5	1.26×10^{-16}	18.9
	2.85	1.10×10^{-16}	17.0
	3	1.12×10^{-16}	17.4
	3.25	9.05×10^{-17}	16.4
	3.5	8.44×10^{-17}	15.4
	3.75	8.30×10^{-17}	14.1
	4	8.31×10^{-17}	14.0
	4.25	8.20×10^{-17}	13.9
	4.5	7.97×10^{-17}	13.1
	4.75	8.64×10^{-17}	13.7
	5	8.46×10^{-17}	13.7
	5.5	9.61×10^{-17}	13.7
	6	1.12×10^{-16}	12.9
	6.5	1.25×10^{-16}	13.0
	7	1.45×10^{-16}	13.1
	7.5	1.58×10^{-16}	12.8
	8.5	1.78×10^{-16}	12.9
	9	2.00×10^{-16}	12.9
	10	2.21×10^{-16}	12.8
	11	2.37×10^{-16}	13.0
	12	2.60×10^{-16}	12.9
	12.5	2.70×10^{-16}	12.9
He^+	1	3.35×10^{-17}	16.6
	1.125	3.46×10^{-17}	16.6
	1.25	4.41×10^{-17}	16.7
	1.375	5.03×10^{-17}	16.6
	1.5	5.86×10^{-17}	16.6
	1.625	6.47×10^{-17}	16.5
	1.75	7.09×10^{-17}	16.6
	1.875	7.82×10^{-17}	16.6
	2	8.68×10^{-17}	16.6
	2.125	9.86×10^{-17}	16.6
	2.25	1.09×10^{-16}	16.6
	2.5	1.00×10^{-16}	16.6
	2.75	1.02×10^{-16}	16.6
	3	9.93×10^{-17}	16.6
	3.125	9.96×10^{-17}	16.6

calculations which assume a simple straight line trajectory for the heavy particles and describe the motion of a single active electron by quantum-mechanical means in the field of both collision partners. Thus, the wavefunction of the active electron is expanded into projectile- and target-centred atomic states as well as into continuum states which build up the basis of the AO-CC calculation. Such a basis describes all inelastic reaction channels like electron capture, target excitation and ionization, but will in fact not be complete. Therefore, the choice of a truncated basis is one of the most critical points, and cross sections have to be checked against variation in basis size and combination of states. All presented cross sections originate from a

Table 2. Composition of the applied datasets with respect to the origin of cross sections for collisions between Li atoms and electrons and protons (cf section 3). Old: data from [9, 18]

e50p31	Electrons: all excitation and all ionization cross sections from CCC calculations [14], except for ionization of Li(2s) [9, 18] and excitation within $n = 4$ shell [18]
	Protons: old
e31p50	Electrons: old
	Protons: all new AO-CC data
e50p50	Electrons: as in e50p31
	Protons: as in e31p50
e51p50	Electrons: as in e50p50, except Li(2s $\rightarrow$ 2p) excitation [9]
	Protons: as in e31p50
e52p50	Electrons: as in e51p50, except all ionization cross sections [9]
	Protons: as in e31p50
e52p51	Electrons: as in e51p50
	Protons: as in e31p50 except electron loss from Li(2s) [11]

large-scale AO-CC calculation with 65 projectile- and 64 target-centred states, which include all atomic states on both centres with principal quantum numbers $n \leqslant 4$. A more detailed description of the theoretical approach can be found in [12].

AO-CC calculations deliver excitation cross sections which have to be transformed into the respective emission cross sections by applying equations (1) and (2) (branching ratios taken from [17]) in order to be comparable with experimental data:

$$\sigma(2p \rightarrow 2s) = \sigma(2p) + \sigma(3s) + 0.76\sigma(3p) + \sigma(3d) + 0.89\sigma(4s) + 0.45\sigma(4p) + 0.94\sigma(4d) + \sigma(4f) \quad (1)$$

$$\sigma(3d \rightarrow 2p) = \sigma(3d) + 0.20\sigma(4p) + \sigma(4f). \quad (2)$$

Experimental and calculated data agree very well in the investigated energy region (cf figure 3) which proves that the AO-CC approach is capable of delivering accurate cross sections even for non-dominant inelastic transitions as the Li(2s $\rightarrow$ 3d) excitation. Comparison of theory and experimental cross sections for the dominant reaction channels like electron capture and Li(2s $\rightarrow$ 2p) excitation (both of them are by about one order of magnitude larger than the Li(2s $\rightarrow$ 3d) excitation cross section) can be found in [10] and [12]. This excellent agreement between the AO-CC results and the now available experimental data for various inelastic transitions in neutral Li enhanced the level of confidence for all other theoretical cross sections necessary for the update of the collision-radiative model, especially in cases where no explicit experimental verification was feasible.

3. Modelling of a fast Li atom beam interacting with the edge plasma

In this section we will present experimental and calculated results regarding the composition of a Li diagnostic beam at IPP Garching with respect to the population of Li(nl) states. In particular, we will discuss the effects of the new cross section data on the reconstruction of plasma electron as well as impurity ion densities.

Description of used atomic datasets. New close-coupling calculations for all inelastic processes of Li(nl) by electron and proton impact have recently become available [10, 14] and are the basis for the new database described in detail by Schweinzer *et al* [10]. As already mentioned the most important change concerns the excitation cross section by proton impact (cf section 2). These cross sections are, in general, considerably reduced for excitation processes

to higher excited states. However, for electron impact the new cross section data originating from the convergent close coupling (CCC) method [14] also become smaller in the region around the threshold in comparison to the data of [9], whereas for higher electron impact energies (the region where the Born approximation is valid) no changes occur. The dataset e50p50 (cf table 2) merges these theoretical data of both close coupling methods for electron and proton impact respectively with the exception of the Li(2s) ionization cross section. In this case the experimental data of [9] are preferred.

We have also produced 'mixed' datasets containing 'old' data for electrons and 'new' data for protons (e31p50) and *vice versa* (e50p31) in order to see which changed dataset has more influence on the results of beam modelling.

Furthermore, we have generated datasets (i.e. datasets e5xp5y ($x = 0$–2; $y = 0, 1$) in table 2) which contain the same atomic data (based on e50p50) for most processes and differ only in those cases for which, in addition to the theoretical data, accurate experimental cross sections are available. For example the dataset e51p50 contains the experimental cross section for the Li(2s–2p) electron excitation process instead of that from the convergent close coupling calculation. Thus using this different dataset permits us to estimate the uncertainty of modelling results due to the remaining error bars of the atomic cross section data. From the point of view of critical data assessment, the dataset e51p50 is regarded as the recommended one and used in all model calculations where the used dataset is not stated. The modelling based on the new datasets delivers populations for 10 Li states (2s, 2p, 3s, 3p, 3d, 4s, 4p, 4d, 4f, Li^+) whereas results from the old database do not contain the 4f state. An overview of all datasets is given in table 2.

3.1. Population of higher excited states

Li atoms occupy the Li(2s) ground state when extracted from the beam injector, but higher states become increasingly populated with increasing penetration depth, and finally all Li atoms become ionized. The most relevant excited state is Li(2p) which has a maximum population fraction of around 15%, with higher states accounting for about 1% or less. Since inaccurately modelled cascade contributions from higher states to the Li I(2p $\rightarrow$ 2s) emission could lead to errors in the electron density reconstruction, and charge-exchange cross sections are much higher for higher excited states, the determination of impurity ion densities could be affected. For these reasons the population of excited states within the Li beam have to be known along the whole penetration length.

In addition, the question of how accurately the population of higher excited states can be modelled and how large the atomic data base has to be, is of considerable interest for atomic beam diagnostic methods of the next generation like a fast He beam. This method will rely on modelling exactly He I($n \geqslant 3$). Therefore, the experience gained with investigations for a Li beam will considerably help the development of such future diagnostic beams.

On both large fusion experiments at IPP Garching measurements have been performed for the population ratios of Li(3d/2p), Li(4s/2p) and Li(4d/2p) states. These results have been compared to the results of the Li beam modelling which has been based on various data sets in order to recognize the relevant changes.

The experimental method will only be outlined roughly here. The diagnostic set-ups on both experiments consist of two separate optical systems each. One of them is dedicated to the measurement of electron densities by collecting Li I(2p $\rightarrow$ 2s) line radiation (Li impact excitation spectroscopy (Li-IXS)), the other one to the investigation of the characteristic line emission of plasma impurities following electron capture from the Li beam atoms (Li charge-exchange spectroscopy (Li-CXS)). These two systems can be cross-calibrated by simultaneous

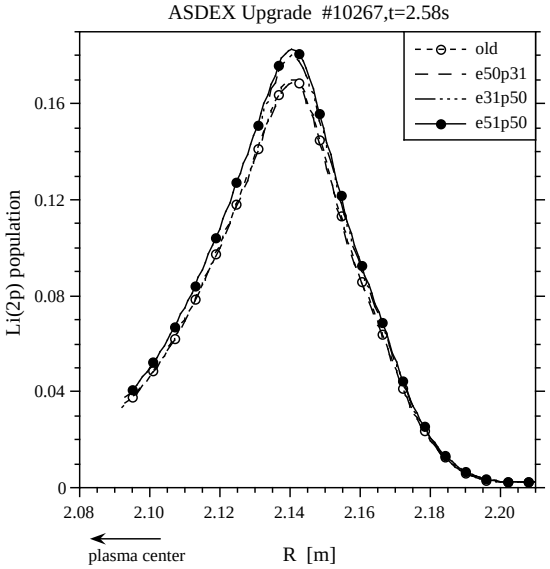

Figure 4. The calculated Li(2p) population as a function of main plasma radius when utilizing different versions of the database (cf table 2 for details on the new database). The main increase is caused by the new proton excitation impact cross sections.

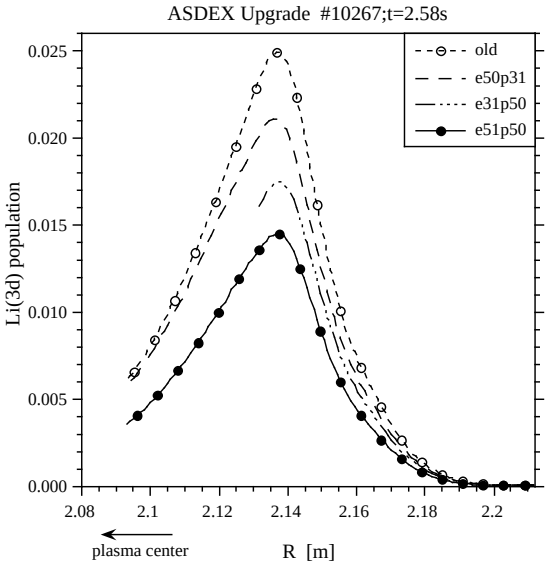

Figure 5. Calculated Li(3d) populations decrease by a factor of two when utilizing the new database (cf table 2 for details on the new database). The main contribution is caused by the new proton impact cross sections.

measurements of the Li I(2p $\rightarrow$ 2s) spectral line in the same discharge. Consequently, the thereby obtained instrumental factors allow the determination of other Li(nl) populations if during the following discharges the Li-IXS set-up (photomultipliers with interference filters) is used to record the Li I(2p $\rightarrow$ 2s) emission, while the Li-CXS set-up (spectrometer and CCD camera) is applied for observation of other Li I lines of interest. The diagnostic systems on

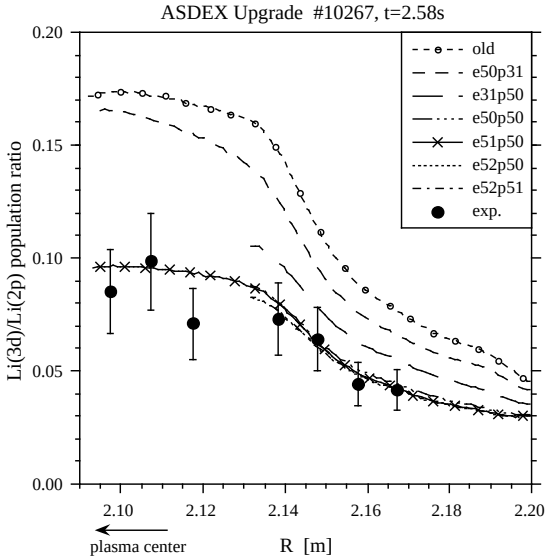

Figure 6. Experimental and calculated results for Li(3d)/Li(2p) population ratios in an ASDEX Upgrade discharge. While separate utilization of new data for electron and ion impact each lower the calculated ratio to some extent, all datasets with variations of new data for both electrons and protons deliver very similar results (cf table 2 for details on the new database).

ASDEX Upgrade and W7-AS operate at different beam energies of 35 and 48 keV, respectively. Further details on the experimental set-ups have been given in [7].

3.1.1. Results. As a first step the effects of new cross sections for electron and proton impact have been investigated. Figures 4 and 5 show that the Li(2p) population slightly increases by around 5% while the Li(3d) population decreases by almost a factor of two when utilizing the new database. Populations of all other Li($3 \leqslant n \leqslant 4$) states also decrease by factors of about two (not shown).

Population ratios of Li(3d) and Li(2p) states have been determined experimentally and from calculations for various plasma discharges in a wide range of densities on both fusion devices. The agreement between experimental and calculated results has generally become much better than with the old database (figure 6). In addition, ratios of Li(4s/2p) and Li(4d/2p) populations have also been determined on WENDELSTEIN 7 AS (figure 7). In the case of Li(4s), the new beam modelling agrees satisfactorily with experimental findings. Li(4d) results still deviate due to insufficient consideration of further excited states (e.g. $n = 5$ shell) in the beam modelling (cf section 4).

3.2. Implications for the reconstruction of plasma electron density

Whereas the populations of higher excited states change considerably when utilizing the new cross section data, reconstructed electron densities are affected to a much smaller extent. This can be anticipated by comparing figures 4 and 5, which show increased Li(2p) and decreased Li(nl; $n \geqslant 3$) populations roughly cancelling each other. Due to the differences in the datasets mentioned above, the reconstructed densities give a good estimate for the remaining error in the method caused by uncertainties in the atomic database. Generally speaking, electron densities calculated with the old database are about 5% lower than densities calculated with

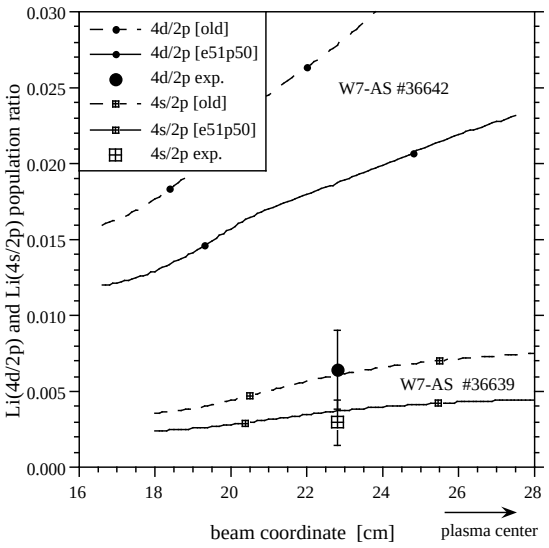

Figure 7. Experimental and calculated results for Li(4s)/Li(2p) and Li(4d)/Li(2p) population ratios in WENDELSTEIN 7 AS discharges. In the case of 4s the agreement is good, especially when considering the very low fraction of Li(4s) population. The remaining deviation between present 10-state modelling and experimental results is most probably caused by neglecting $n = 5$ states in the beam modelling (cf section 4).

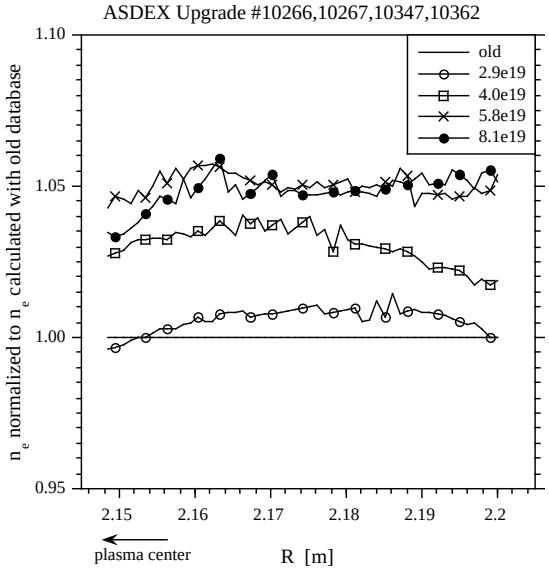

Figure 8. Comparison of reconstructed electron densities when utilizing old and new (i.e. e51p50 from table 2) datasets for discharges with different average density (n_e(DCN) per m^3). While there is no significant change for low plasma density, results are higher by up to 5% for medium and high plasma densities.

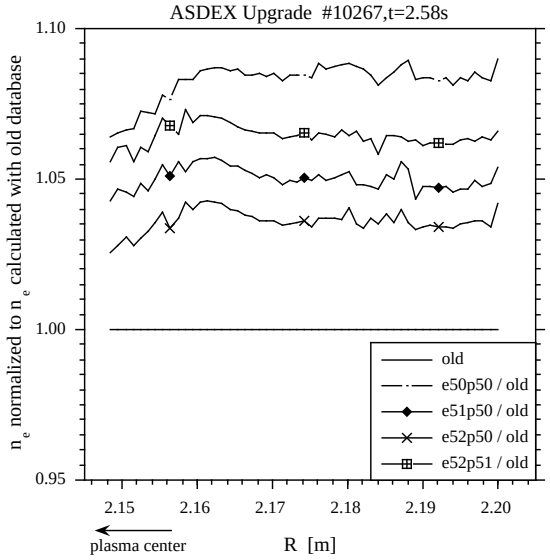

Figure 9. Reconstructed electron densities normalized to the results from the old database in a medium plasma density discharge ($n_e(\mathrm{DCN}) = 5.8 \times 19\ \mathrm{m}^{-3}$). All new datasets deliver somewhat higher densities than the old database, while the differences between calculations involving different new datasets are quite smaller.

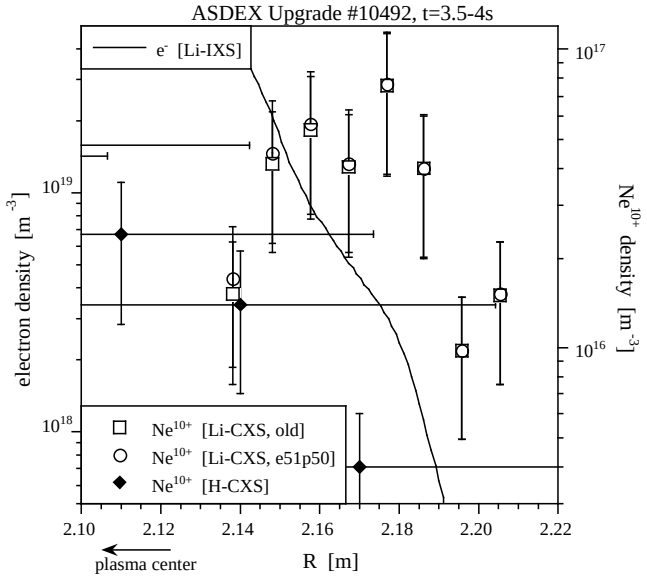

Figure 10. Radial profiles of electron and Ne^{10+} densities. According to the new beam modelling, effective emission cross sections have decreased considerably, leading to measured Ne^{10+} densities up to 15% higher. This picture also demonstrates the value of Li beam edge plasma spectroscopy since the spatial resolution of Li-CXS data is much better than for similar measurements carried out with the hydrogen heating beams.

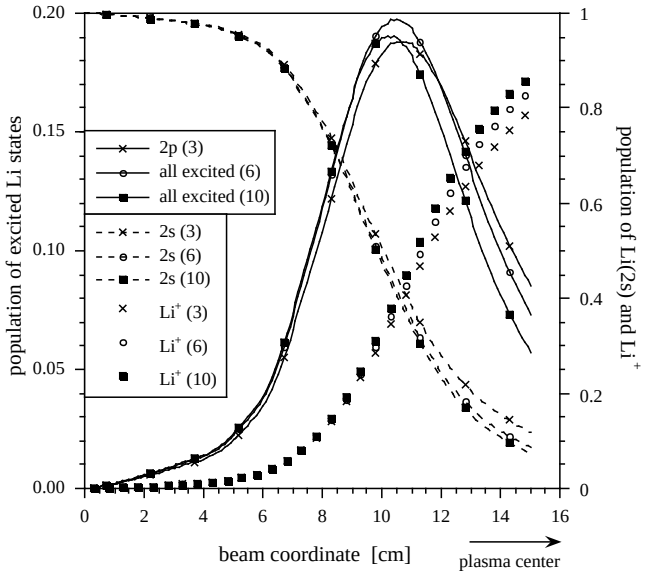

Figure 11. Comparison of Li beam composition for three, six and 10 Li states included in the collisional radiative model under the assumption of a given plasma density and temperature profile. All populations of excited states are added together (cf left scale). In addition, the radial profiles of Li(2s) and Li^+ are plotted (cf right scale). For further details see text.

the other datasets (figure 8), with the exception of very low densities for which there is no unambiguous change. While in most cases there is a clear difference between results obtained with the old and any of the new datasets, results from the various new datasets differ only by a few per cent (figure 9). This indicates that the method has now reached a status where any further refinement of the database will no longer affect the reconstructed electron densities in a significant way.

3.3. Implications for the determination of impurity ion densities

The local composition of diagnostic Li beams is of particular importance for the evaluation of plasma impurity densities since the cross sections for single electron capture from Li(nl) atoms strongly depend on the initial Li(nl) state. Due to the now much smaller Li(nl; $n \geqslant 3$) populations we found a decrease of effective emission cross sections for charge-exchange processes and consequently an increase in reconstructed impurity ion densities (a typical example is given in figure 10).

4. Are 10 Li-states sufficient for accurate beam modelling?

In figure 11 we compare Li beam compositions as calculated by three different models, including three, six and 10 Li states (equivalent to inclusion of the $n = 2$, 3 and 4 shells), respectively, the Li^+ state always being included. All three models assume the same plasma density profile and start solving the Li beam rate equations at $z = 0$ (z is the beam coordinate) with the boundary conditions Li(2s) $= 1$, Li($nl > 2$s) $= 0$ (beam energy 35 keV). Populations of all excited states are added to a single profile. As shown in figure 11, the gross population of excited states does not change dramatically with the size of the model which means that the

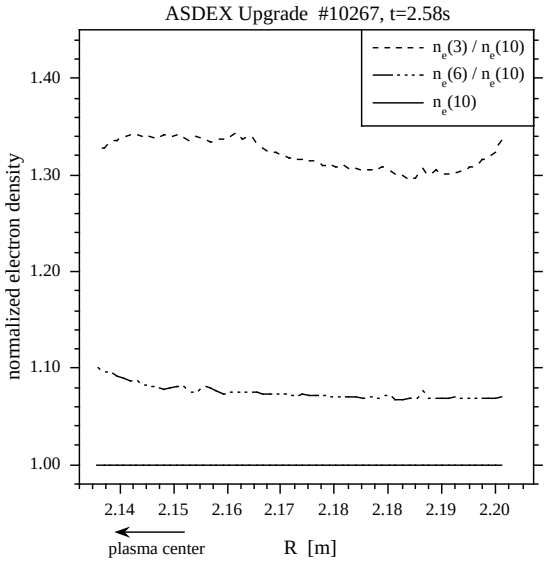

Figure 12. Ratios of electron densities reconstructed with Li beam models containing three, six and 10 states. The reconstruction of electron densities converges with calculated electron densities decreasing when more Li(nl) states are included.

population of higher excited shells is dominantly due to stepwise excitation from neighbouring lower shells and not from the ground state. In other words, adding more Li(nl) states to the model may change the fraction of a specific excited state, but to a much lesser extent the gross population of all excited states together. This behaviour is due to the dramatic decrease of excitation cross sections with increasing excitation energy.

A higher number of states in the model leads to increased attenuation of the beam as can be seen by comparing Li^+ profiles from the three models (cf figure 11). This effect is due to increasing cross sections for electron loss (ionization + charge transfer in collisions with protons) with decreasing Li(nl) ionization potential.

The inclusion of a further shell ($n = 5$) will therefore probably decrease the population of the $n = 4$ states by 20–25%, leading to an estimated population of the $n = 5$ shell by a factor of three to four lower than for the $n = 4$ shell. Because of the increased electron loss cross sections for the $n = 5$ states, this additional population will increase the attenuation. However, the effect on the gross attenuation will be smaller than for the step from the six-state to the 10-state model, because the electron loss cross sections scale approximately with the principal quantum number squared. From the change in beam attenuation by 3.5% for the step from the six-state to the 10-state model, we extrapolate a further increase of attenuation of $\leqslant 2\%$.

For a given Li(2p) profile and reconstruction of the density from the respective emission with different numbers of Li(nl) states involved, the obtained plasma density will decrease with an increasing number of states (cf figure 12). Therefore, plasma density profiles from Li-IXS with only a limited number of Li(nl) states being taken into account have to be considered as upper limits for the actual density. From our experience with the comparison of such derived Li-IXS profiles with other independent n_e measurements we estimate that this systematic error has become less than 5% in the case of a 10-state model at beam energies below 50 keV.

At considerably higher beam energies, however, the population fraction of $n \geqslant 3$ states will increase, which most probably will lead to less convergence of density results when the

same number of neutral states in the reconstruction algorithm is included. Li beam diagnostic systems with beam energies up to 100 keV are currently being discussed with respect to next step devices (e.g. W7-X stellarator) in order to increase the penetration depth, thus enlarging the accessible plasma edge region.

5. Summary

We have investigated the state composition of diagnostic lithium beams along their way through typical fusion edge plasmas. Extensive atomic orbital-close coupling calculations have been performed for determination of Li(nl; $n \leqslant 4$) proton impact excitation cross sections, and comparison with experimental data for the most relevant excited states Li(2p) and Li(3d) show very good agreement. The new data provide a considerable upgrade of our database for the modelling of the Li beam attenuation. With this new database, the Li beam attenuation is now satisfactorily described, and respective measurements constitute a useful and reliable method for the investigation and characterization of the fusion edge plasma region.

Acknowledgments

This work has been performed within Association EURATOM-OEAW and was supported by Friedrich Schiedel-Stiftung für Energietechnik.

References

[1] McCormick K, Fiedler S, Kocsis G, Schweinzer J and Zoletnik S 1997 *Fusion Eng. Design* **34/35** 125
[2] Wolfrum E, Aumayr F, Wutte D, Winter HP, Hintz E, Rusbüldt D and Schorn R P 1993 *Rev. Sci. Instrum.* **64** 2285
[3] Schweinzer J, Wolfrum E, Aumayr F, Pöckl M, Winter HP, Schorn R P, Hintz E and Unterreiter A 1992 *Plasma Phys. Control. Fusion* **34** 1173
[4] Aumayr F, Schorn R P, Pöckl M, Schweinzer J, Wolfrum E, McCormick K, Hintz E and Winter HP 1992 *J. Nucl. Mater.* **196–198** 928
[5] Schorn R P, Hintz E, Rusbüldt D, Aumayr F, Schneider M, Unterreiter E and Winter HP 1991 *Appl. Phys* B **52** 71
[6] Schorn R P, Wolfrum E, Aumayr F, Hintz E, Rusbüldt D and Winter HP 1992 *Nucl. Fusion* **32** 351
[7] Brandenburg R, Fiedler S, McCormick K, Petravich G, Aumayr F, Winter HP, Schweinzer J and the W7-AS Team 1997 *Europhys. Conf. Abstr.* **21A** 477
[8] Fiedler S, Brandenburg R, Baldzuhn J, McCormick K, Aumayr F, Schweinzer J, Winter HP and the W7-AS Team 1998 *J. Plasma Fusion Res. SERIES* **1** 287
[9] Wutte D, Janev R K, Aumayr F, Schneider M, Schweinzer J, Smith J J and Winter HP 1997 *At. Nucl. Data Tables* **65** 155
[10] Schweinzer J, Brandenburg R, Bray I, Hoekstra R, Aumayr F, Janev R K and Winter HP 1999 *At. Nucl. Data Tables* at press
[11] Aumayr F, Fehringer M and Winter HP 1984 *J. Phys. B: At. Mol. Phys.* **17** 4185
[12] Brandenburg R, Schweinzer J, Aumayr F and Winter HP 1998 *J. Phys. B: At. Mol. Opt. Phys.* **31** 2585
Nielsen S E, Hansen J P and Dubois A 1990 *J. Phys. B: At. Mol. Opt. Phys.* **23** 2595
[13] Wutte D, Leitner M and Winter HP 1994 *Rev. Sci. Instrum.* **65** 1094
[14] Bray I 1997 Private communication
[15] Hansen J P, Kocbach L, Synnes S A, Wang J B and Dubois A 1998 *Phys. Rev.* A **57** R4086
[16] Aumayr F and Winter HP 1985 *J. Phys. B: At. Mol. Phys.* **18** L741
[17] Wiese W L, Smith M W and Glennon B M 1966 *Atomic Transition Probabilities* (Washington, DC: US Govt Printing Office)
[18] Janev R K, Smith J J, Aumayr F, Wutte D, Schneider M, Winter HP and Schweinzer J 1993 Atomic collision database for Li beam interaction with fusion plasmas *IAEA Report* INDC(NDS)-267